Godunov method for multiprobe cryosurgery simulation with complex-shaped tumors

D. Tarwidi

Citation: AIP Conference Proceedings **1707**, 060002 (2016); doi: 10.1063/1.4940855
View online: http://dx.doi.org/10.1063/1.4940855
View Table of Contents: http://scitation.aip.org/content/aip/proceeding/aipcp/1707?ver=pdfcov
Published by the AIP Publishing

Godunov Method for Multiprobe Cryosurgery Simulation with Complex-Shaped Tumors

D. Tarwidi

Department of Computational Science, School of Computing, Telkom University
Jalan Telekomunikasi Terusan Buah Batu, Bandung 40257, Indonesia
dedetarwidi@telkomuniversity.ac.id

Abstract. Cryosurgery is a technique to eradicate abnormal biological tissues by freezing. The objective of cryosurgery is to maximize cryoinjury of tumor tissues while at the same time minimizing cryoinjury to the surrounding healthy tissues. The location and number of cryoprobes are important factors to obtain optimal cryosurgery in complex-shaped tumors. This paper presents multiprobe cryosurgery simulation with optimal cryoprobes location in target region. Bubble packing method is used to obtain optimal cryoprobes layout. We consider mathematical model of freezing by bioheat transfer equation in solid (frozen tissue), liquid (unfrozen tissue), and mushy region. This model is referred to as Stefan problem where the location of moving solid-mushy or mushy-liquid interface is not known and it is as part of the solution. We reformulate the bioheat equations into single enthalpy (energy) equation which can resolve the moving boundary between two phases. The first-order of Godunov method is adopted to obtain numerical solution of the phase change problem. This method is easily applied since we only solve one governing equation regardless the moving interface between two phases. For demonstration purposes, multiprobe cryosurgery for lung cancer case with complex geometry is simulated and interpreted. The numerical simulation for three to ten cryoprobes configuration shows that the nine cryoprobes layout has the smallest total defect in this case. The numerical results provide an important information for cryosurgeon before conducting effective cryosurgery protocol.

Keywords: Godunov method; Multiprobe cryosurgery; Bubble packing, Stefan problem; Enthalpy formulation; Numerical simulation
PACS: 02.60.Cb, 02.70.Bf

INTRODUCTION

Cancer has become one of the most frightening disease in the world. Each year globally, million of people died because of cancer. According to the world health organization (WHO), in 2012, about 8.2 million people died from cancer with 1.59 million of which caused by lung cancer. There are several medical treatments to cure cancer, among others are chemotherapy, radiotherapy, surgery, or combination of these three methods. Cryosurgery is one of the surgical technique to destroy tumor tissues by inserting extremely cold temperature into tumor area through a device called cryoprobe. Cryosurgery is formerly developed for single probe. However, due to the complex geometry of tumors, cryosurgery is developed to multiple cryoprobes [1]. In multiprobe cryosurgery problem, the number of cryoprobes used and where to place them into the tumor area are important factors to perform a successful cryosurgery.

The multiprobe cryosurgery procedure can be described as follows. At first, extremely cold temperature which usually provided by liquid nitrogen with temperature $-196\,^{\circ}\mathrm{C}$ is inserted into a predefined target region (illustrated in Fig. 1) through a number of cryoprobes. We assume that at initial, all biological tissues are in liquid phase. However, due to very low-temperature, the region surrounding each cryoprobe forms ice balls. As a result, biological tissue is divided into two regions, namely solid and liquid region. At certain time, the ice balls will merge to form a single ice region which eventually covers the whole target region. Tumors tissue will be damaged if the area of ice has temperature between $0\,^{\circ}\mathrm{C}$ and $-45\,^{\circ}\mathrm{C}$ [2]. The objective of the cryosurgery procedure is to maximize cryoinjury of tumor tissues, while at the same time the surrounding healthy tissue damage is minimized.

There have been several numerical simulations to achieve the objective of cryosurgery. Rossi et al. [2, 3] developed computerized planning tools for multiprobe cryosurgery of prostate tumor. They used bubble packing method and force-field analogy to obtain optimal layout of cryoprobes position. The numerical method used in their numerical simulation was finite difference method and the numerical results were validated by experimental data of phantom material. It showed that the freezing front location from the simulation only differs 0.8 mm from the experimental data. Lung et. al [4] also used force-field analogy to obtain the optimal position of cryoprobes. They showed that this method more efficient than traditional numerical optimization technique. The other techniques for optimizing cryoprobes layout can be found in [5, 6, 7]. Moreover, Chua [1] conducted multiprobe cryosurgery simulation for liver

Proceedings of The 7th SEAMS UGM International Conference on Mathematics and Its Applications 2015
AIP Conf. Proc. 1707, 060002-1–060002-12; doi: 10.1063/1.4940855

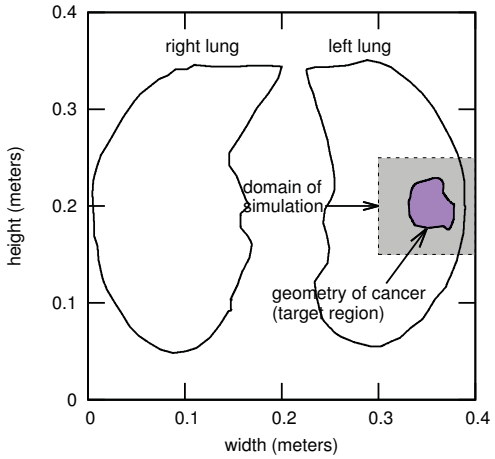

FIGURE 1. Configuration of human lung cancer cryosurgery where the highlighted area is the domain of simulation. Area of lung cancer and healthy left lung are 18.988 cm^2 and 334.605 cm^2 respectively.

tumors with irregularly geometry. But, in the simulation, the cryoprobes position was not optimized. However, the numerical results showed good agreement of up to 5.8% with experimental data. Furthermore, Kumar [8] developed 3D model to study the effect of central probe on the multiprobe cryosurgery process while Wan et. al [9] used finite element model to simulate ice ball evolution in multiprobe cryosurgery.

The mathematical model of cryosurgery process consists of heat transfer in frozen tissue (solid phase), unfrozen tissue (liquid phase), and conservation of energy at mushy region. The mushy region is portion of the area of biological tissue where the phase is in neither solid nor liquid. The governing equation in solid region is derived from heat conduction whereas in liquid region is represented by classical Pennes bioheat transfer equation [10]. This problem is referred to as Stefan problem—i.e. a free boundary problem where boundary between solid-mushy and mushy-liquid move as function of time. There have been many methods developed to solve the Stefan problems, including boundary immobilization method, perturbation method, nodal integral method, heat balance integral method, and enthalpy method. The comparative studies of these methods can be found in [11, 12]. The boundary immobilization method can effectively remove the moving boundary, but unfortunately it needs to solve more complicated equation. In the perturbation method, the position of moving boundary can be transformed into ordinary differential equation but it is hard to solve numerically and it requires symbolics computation. Further, the nodal integral method gives better results but only for small number of interval. The heat balance integral method can produces good results if the boundary conditions are constant but it become more difficult for time-dependent problems. The simple technique that most widely used to solve Stefan problems is enthalpy method [13, 14, 15]. The enthalpy method works by reformulating heat conduction equations in each phase region into single enthalpy (energy) equation. By this formulation, the governing equation is the same regardless the phases so that the standard numerical method for conservation energy such as Godunov method can be easily applied [16].

In this paper, we propose first-order Godunov method to simulate multiprobe cryosurgery with complex-shaped tumors. More detail about Godunov method can be found in [17]. Here, the bubble packing method is adopted to search optimal cryoprobes location. The numerical simulations for multiprobe lung cancer cryosurgery are conducted for three to ten optimal cryoprobes position.

MATHEMATICAL FORMULATION

Let $\Omega \in \mathrm{R}^2$ denotes tissues region which consists of healthy and tumor tissues. At initial, whole tissues region are in liquid phase. When a number of cryoprobes is inserted into target area, tumor tissues begin to freeze so that there is change of phase from liquid to solid. Let Ω_S and Ω_L be solid and liquid phase region respectively and Ω_i is mushy region that separated solid and liquid region. Temperature at position $\mathbf{x} = (x, y) \in \mathrm{R}^2$ and time t is denoted by $T(\mathbf{x}, t)$.

Heat conduction equation in frozen tissues (solid phase) may be expressed as

$$\rho_S c_S \frac{\partial T_S(\mathbf{x},t)}{\partial t} = k_S \left(\frac{\partial^2 T_S(\mathbf{x},t)}{\partial x^2} + \frac{\partial^2 T_S(\mathbf{x},t)}{\partial y^2} \right), \ \mathbf{x} \in \Omega_S, \tag{1}$$

where ρ_S, c_S, and k_S are density, specific heat, and thermal conductivity of frozen tissue respectively. Further, due to the presence of blood perfusion and metabolic rate in unfrozen tissues (liquid phase), the heat conduction equation is represented as Pennes bioheat transfer equation [10]:

$$\rho_L c_L \frac{\partial T_L(\mathbf{x},t)}{\partial t} = k_L \left(\frac{\partial^2 T_L(\mathbf{x},t)}{\partial x^2} + \frac{\partial^2 T_L(\mathbf{x},t)}{\partial y^2} \right) + \omega_b \rho_b c_b \left[T_b - T_L(\mathbf{x},t) \right] + Q_m, \quad \mathbf{x} \in \Omega_L, \tag{2}$$

where ρ_L, c_L, and k_L are density, specific heat, and thermal conductivity of unfrozen tissue respectively. Moreover, ω_b, ρ_b, c_b, T_b, and Q_m are perfusion, density, specific heat, temperature, and metabolic heat generation of blood respectively. More discussion about the Pennes bioheat transfer can be found in [18, 19, 20].

The condition at mushy region follows [1]:

$$\rho_i c_i \frac{\partial T_i(\mathbf{x},t)}{\partial t} = k_i \left(\frac{\partial^2 T_i(\mathbf{x},t)}{\partial x^2} + \frac{\partial^2 T_i(\mathbf{x},t)}{\partial y^2} \right) + \omega_b \rho_b c_b \left[T_b - T_i(\mathbf{x},t) \right] + Q_m + \rho_i L \frac{df_s}{dt}, \quad \mathbf{x} \in \Omega_i, \tag{3}$$

where ρ_i, c_i, and k_i are density, specific heat, and thermal conductivity of tissue in mushy region respectively and L is latent heat of fusion. Here, f_s is solid fraction during phase change:

$$f_s = \begin{cases} 0, & T(\mathbf{x},t) = T_{ml}, \\ 1, & T(\mathbf{x},t) = T_{ms}, \\ \dfrac{T(\mathbf{x},t) - T_{ml}}{T_{ms} - T_{ml}}, & T_{ms} < T(\mathbf{x},t) < T_{ml}, \end{cases} \tag{4}$$

where T_{ms} and T_{ml} are solidus and liquidus temperature, respectively. For the simplicity of the computation, we assume $\rho = \rho_S = \rho_L = \rho_i$.

Boundary conditions at the interface between solid and mushy region can be written as

$$T(\mathbf{x},t) = T_{ms}, \quad \mathbf{x} \in \Gamma_m(t) \tag{5}$$

$$k_s \nabla T_S(\mathbf{x},t) \cdot \mathbf{n}_s = k_i \nabla T_i(\mathbf{x},t) \cdot \mathbf{n}_s, \quad \mathbf{x} \in \Gamma_m(t) \tag{6}$$

where $\mathbf{n}_s$ is the unit normal vector to solid-mushy region interface and $\Gamma_m(t)$ denotes moving boundary. Moreover, boundary conditions at the interface between mushy and liquid region are given by

$$T(\mathbf{x},t) = T_{ml}, \quad \mathbf{x} \in \Gamma_m(t) \tag{7}$$

$$k_i \nabla T_i(\mathbf{x},t) \cdot \mathbf{n}_l = k_L \nabla T_L(\mathbf{x},t) \cdot \mathbf{n}_l, \quad \mathbf{x} \in \Gamma_m(t) \tag{8}$$

where $\mathbf{n}_l$ is the unit normal vector to mushy-liquid region interface. The equation (1) – (8) are mathematically referred to as Stefan problem.

COMPUTATIONAL METHODS

In this section, the first-order of Godunov method is presented in brief. Besides, we formulate minimization of total defect to measure effectiveness of cryosurgery process. At the end of this section, the bubble packing method is briefly discussed.

Godunov Method

Interface position of solid-mushy and mushy-liquid region at each time is a priori unknown. As consequence, the equation (1) – (8) can not be directly solved. A technique to solve such problem is to transform the heat conduction

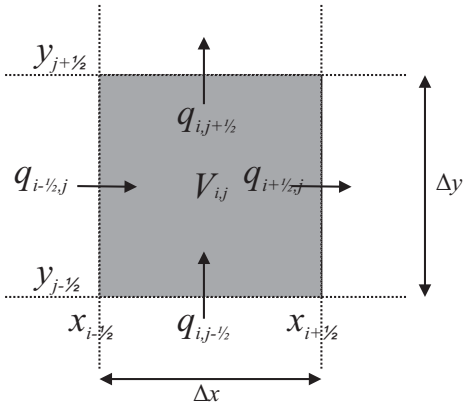

FIGURE 2. Control volume V_{ij} in 2D domain.

equations of solid, liquid, and mushy region into enthalpy equation. In the enthalpy form, the interface between solid-mushy and mushy-liquid region is no longer taken into account in computation so that the numerical scheme in term energy conservation such as Godunov method can be easily applied.

Suppose $E(\mathbf{x},t)$ denotes the enthalpy per unit area at position $\mathbf{x}$ and time t, the sum of sensible and latent latent can be written as [21, 22]

$$E(\mathbf{x},t) = \begin{cases} \rho c_S \left[T(\mathbf{x},t) - T_{ms}\right], & T(\mathbf{x},t) < T_{ms} \quad \text{(solid region)}, \\ \rho \left(\frac{1}{2}\left(c_s + c_l\right) + \dfrac{L}{T_{ml} - T_{ms}} \right) \left[T(\mathbf{x},t) - T_{ms}\right], & T_{ms} \le T(\mathbf{x},t) \le T_{ml} \quad \text{(mushy region)}, \\ \rho L + \frac{1}{2}\rho\left(c_s + c_l\right)\left(T_{ml} - T_{ms}\right) + \rho c_l \left[T(\mathbf{x},t) - T_{ml}\right], & T(\mathbf{x},t) > T_{ml} \quad \text{(liquid region)}. \end{cases} \tag{9}$$

The Godunov method for solving the Stefan problem can be briefly described as follows [16]. At first, we discretize the domain of simulation by finite volume discretization. Let $0 \le x \le l_1$, $0 \le y \le l_2$ be two-dimensional domain of biological tissue, in this case, $l_1 = l_2 = 0.1$ m. The domain $[0,l_1]$ and $[0,l_2]$ are divided into M_1 and M_2 subintervals respectively with length of subinterval $\Delta x = l_1/M_1$ and $\Delta y = l_2/M_2$. Area inside $V_{i,j} = [x_{i-1/2}, x_{i+1/2}] \times [y_{j-1/2}, y_{j+1/2}]$ is defined as control volume (illustrated in Fig. 2) where $x_{i-1/2}$ is a node between x_{i-1} and x_i. Thus, there are $M_1 M_2$ control volumes. The conservation of energy in each control volume $V_{i,j}$ can be expressed as

$$\int_{V_{i,j}} \left[E(\mathbf{x}, t+\Delta t) - E(\mathbf{x},t)\right] \mathrm{d}A = \int_t^{t+\Delta t} \int_{\partial V_{i,j}} -\mathbf{q}\cdot\hat{\mathbf{n}}\, \mathrm{d}S\, \mathrm{d}t, \tag{10}$$

where $-\mathbf{q}\cdot\hat{\mathbf{n}}$ is heat flux into the area $V_{i,j}$ across its boundary $\partial V_{i,j}$, $\hat{\mathbf{n}}$ being the outgoing unit normal to $\partial V_{i,j}$.

The explicit scheme in two-dimensional domain of (10) based on Godunov method is

$$E_{i,j}^{n+1} = E_{i,j}^n + \frac{\Delta t}{\Delta x}\left[q_{i-1/2,j}^n - q_{i+1/2,j}^n\right] + \frac{\Delta t}{\Delta y}\left[q_{i,j-1/2}^n - q_{i,j+1/2}^n\right] + \Delta t\, \omega_b \rho_b c_b \left[T_b - T_{i,j}^n\right] + \Delta t\, Q_m, \tag{11}$$

where

$$q_{i-1/2,j} = \frac{T_{i-1,j} - T_{i,j}}{R_{i-1/2,j}},\ R_{i-1/2,j} = \frac{\Delta x}{2}\left(\frac{1}{k_{i-1,j}} + \frac{1}{k_{i,j}}\right),\ q_{i,j-1/2} = \frac{T_{i,j-1} - T_{i,j}}{R_{i,j-1/2}},\ R_{i,j-1/2} = \frac{\Delta y}{2}\left(\frac{1}{k_{i,j-1}} + \frac{1}{k_{i,j}}\right). \tag{12}$$

Temperature in each control volume $V_{i,j}$ is obtained by substituting (9) into (11) and reformulating the equation into enthalpy term—viz.

$$T_{i,j}^{n+1} = \begin{cases} T_{ms} + \dfrac{E_{i,j}^{n+1}}{\rho c_s}, & E_{i,j}^{n+1} < 0 \\ T_{ms} + \dfrac{E_{i,j}^{n+1}}{\frac{1}{2}\rho(c_s+c_l) + \dfrac{\rho L}{T_{ml}-T_{ms}}}, & 0 \le E_{i,j}^{n+1} \le \rho L + \frac{1}{2}\rho(c_s+c_l)(T_{ml}-T_{ms}) \\ T_{ml} + \dfrac{E_{i,j}^{n+1} - \rho L - \frac{1}{2}\rho(c_s+c_l)(T_{ml}-T_{ms})}{\rho c_l}, & E_{i,j}^{n+1} > \rho L + \frac{1}{2}\rho(c_s+c_l)(T_{ml}-T_{ms}). \end{cases} \tag{13}$$

The analytical solution of (1) – (8) is available for one-dimensional case but without involving blood perfusion and metabolic heat generation. In our previous works [16], we calculated the error of Godunov scheme against its analytical solution. It revealed that the numerical solution of one-dimensional Stefan problem using Godunov method confirmed the analytical solution.

Since the explicit scheme is used for time integration, the numerical method is conditionally stable. The stability of internal nodes of (11) but without perfusion and heat generation of blood term can briefly be derived as follows. We assume that there is only plain heat conduction occurs in the domain of interest or we can say that the energy is simply the sensible heat. As consequence, the specific heat is independent of temperature, so that instead of (9), the energy term in control volume $V_{i,j}$ can be written as

$$E_{i,j}^{n} = \rho c_j \left(T_{i,j}^{n} - T_{ref}\right), \tag{14}$$

where T_{ref} being some convenient reference temperature.

Let suppose the thermal conductivity and specific heat are constant, $k_j = k$, $c_j = c$. Now, substitute (12) and (14) into (11), yields

$$T_{i,j}^{n+1} = T_{i,j}^{n} + \frac{\alpha\Delta t}{\Delta x^2}\left(T_{i-1,j}^{n} - 2T_{i,j}^{n} + T_{i+1,j}^{n}\right) + \frac{\alpha\Delta t}{\Delta y^2}\left(T_{i,j-1}^{n} - 2T_{i,j}^{n} + T_{i,j+1}^{n}\right) \tag{15}$$

where $\alpha = k/(\rho c)$. Without loss of generality, we assume $\Delta x = \Delta y$ and

$$\mu = \frac{\alpha\Delta t}{\Delta x^2}, \tag{16}$$

then (15) may be written as

$$T_{i,j}^{n+1} = (1-4\mu)T_{i,j}^{n} + 2\mu\left(T_{i-1,j}^{n} + T_{i+1,j}^{n} + T_{i,j-1}^{n} + T_{i,j+1}^{n}\right). \tag{17}$$

The condition for stability is that $1-4\mu \ge 0$, known as the Courant-Friedrichs-Lewy (CFL) conditions:

$$\Delta t \le \frac{1}{4}\frac{\Delta x^2}{\alpha}. \tag{18}$$

Furthermore, since Δx and Δy may be different in the computation and in our case the value of α depends on phases, then (18) may be written as

$$\Delta t \le \frac{1}{4}\frac{\min\left\{\Delta x^2, \Delta y^2\right\}}{\alpha_{max}}, \quad \alpha_{max} = \max\left\{\frac{k_s}{\rho_s c_s}, \frac{k_l}{\rho_l c_l}\right\}. \tag{19}$$

Minimization of Defect Region

We know that the aim of cryosurgery is to maximize cryoinjury of target region while minimizing the destruction of healthy tissues. For demonstration purposes, we assume that to ensure tumors ablation, the temperatures must be

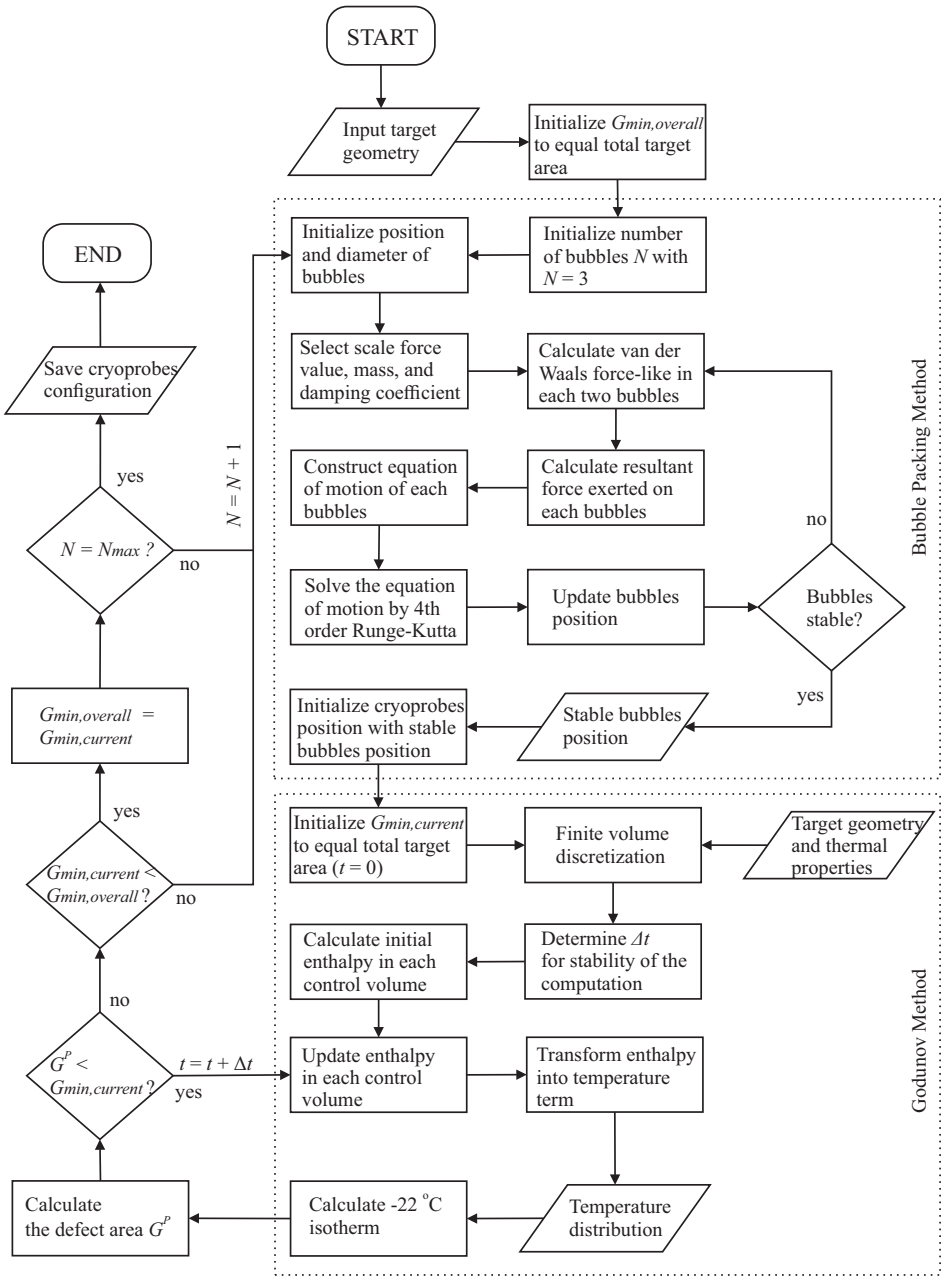

FIGURE 3. Multiprobe cryosurgery planning algorithm using bubble packing method for optimizing cryoprobes position and Godunov method for the solution of Stefan problem: N is the number of cryoprobes, $N = 3, 4, \ldots, N_{max}$; $N_{max} = 10$ is the maximum number of cryoprobes being tested; G^p is the objective function given in (20) at time level p; $G_{min,current}$ is the minimum of defect function calculated up to time level p; $G_{min,overall}$ is the minimum of defect function from all cryoprobes configurations.

below $-22°$C [3]. Now the objective is to lower temperature of entire tumors area below $-22°$C while resisting the temperature of surrounding healthy tissues above this temperature. In other words, the objective is to minimize area inside target region where the temperature is above $-22°$C and also minimize area outside target region where the temperature is below $-22°$C. If we define internal defect is area inside target region that has temperatures above

-22°C and external defect is area outside target region that has temperature below -22°C then the objective function can be formulated as [3]:

$$G = \int_A w\,dA; \quad w = \begin{cases} 1, & -22\ ^{\circ}\text{C} < T \quad \text{interior to the target region} \\ 0, & T \leq -22\ ^{\circ}\text{C} \quad \text{interior to the target region} \\ 1, & T \leq -22\ ^{\circ}\text{C} \quad \text{exterior to the target region} \\ 0, & -22\ ^{\circ}\text{C} < T \quad \text{exterior to the target region,} \end{cases} \tag{20}$$

where G is called defect function and A is area of the domain under consideration. This leads us to minimization problem—i.e. minimizing the defect function.

Bubble Packing Method

Bubble packing is a method to search an even distribution of a number of objects into a domain with a specific geometry. As an example, the bubble packing is used as mesh generation in finite element analysis. More discussion about the bubble packing method can be found in [23]. In this study, bubble packing is used to search an optimal position of a number of cryoprobes that will minimize total defect region in (20). Suppose that there is a number of 2D bubbles with the center point of $\mathbf{x} = (x_j, y_j)$. Each bubble inside the domain moves following the van der Waals-like force. The bubbles motion consist of attraction and repulsion force, where the attraction force occurs when two bubbles have great distance while the repulsion force occurs when two bubbles have short enough distance. The van der Waals-like force between two bubbles is given by [24]

$$f(\lambda) = \begin{cases} k_0 \left(\frac{5}{4}\lambda^3 - \frac{19}{8}\lambda^2 + \frac{9}{8}\right), & 0 \leq \lambda \leq 1.5 \\ 0, & \lambda > 0, \end{cases} \tag{21}$$

where λ is the ratio between the actual distance to the desired distance between two bubbles, and k_0 is parameter to scale force value.

In the computation, we consider fix and free bubbles. Fix bubbles are dummy bubbles which are placed at boundary of domain and it can not move while free bubbles move according to van der Waals force. The dummy bubbles are created to prevent free bubbles moves outside the domain. Further, The equation of motion for the bubble system is given by Newton's 2nd Law:

$$m\frac{d^2\mathbf{x}_i(t)}{dt^2} + c\frac{d\mathbf{x}_i(t)}{dt} = \mathbf{F}_i(t) \tag{22}$$

where m is mass, c is damping coefficient, and $\mathbf{F}_i$ is the resultant force exerted on the ith bubble. Moreover, equation (22) can be solved by reformulating it to a system of first-order ordinary differential equation and numerically solved by the fourth-order of Runge-Kutta method. The equation is iterated until stable bubbles position is attained. The number of iterations for a number of bubbles depends on selection of physical parameter such as mass, damping coefficient, force value, and initial distance of inter bubble position. The multiprobe cryosurgery planning algorithm using bubble packing method for optimizing cryoprobes position and Godunov method for the solution of Stefan problem is shown in the flow chart in Fig. 3.

RESULTS AND DISCUSSION

Here, we discuss optimal cryoprobes position obtained from bubble packing method. These optimal positions are used to calculate total defect of target region. We also analyze and interpret the numerical results of multiprobe cryosurgery simulation for three to ten cryorprobes configuration.

Optimal Cryoprobes Position

Before performing cryosurgery using several cryoprobes, the position of the cryoprobes need to be determined by cryosurgeon. Here, bubble packing method is used to obtain optimal cryoprobes position that will maximize the cancerous tissue damage, but minimizing healthy tissue damage. In this study, numerical simulation to obtain the

TABLE 1. Number of iteration for given initial bubbles position with diameter of bubbles.

Number of bubbles	Diameter of bubbles (m)	Number of iterations
3	0.0210	132
4	0.0185	5882
5	0.0160	937
6	0.0149	21797
7	0.0147	5444
8	0.0147	6869
9	0.0130	21329
10	0.0126	4317

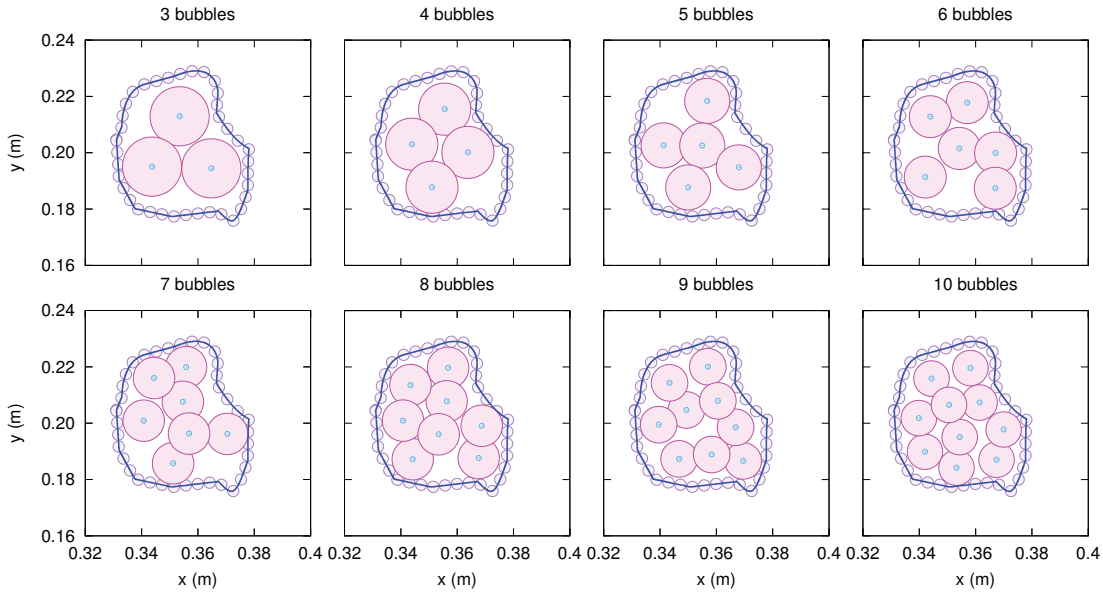

FIGURE 4. Optimal bubbles position using bubble packing method.

optimal location is performed for three to ten cryoprobes. Table 1 shows the simulation results for the number of iterations and the diameter of each bubble using bubble packing method. It can be seen that the fewest iteration is obtained for three bubbles—i.e. 132 iterations while the most iteration is obtained for six bubbles—i.e. 21797 iterations. The number of iterations is mostly determined by the initial bubbles position and diameter of bubbles. If the initial bubbles position is stable enough then the number of iterations will be less. In contrast, if the initial bubbles position is very unstable, the number of iterations will be more and more. The bubble diameters are used in this bubble packing simulation should be adjusted so that the combined area of bubbles as widely as possible but still within the target region.

The position of stable bubbles obtained from the simulation is displayed by Fig. 4. As can be seen from the figure, the bubbles are allowed to overlap with a certain ratio with the aim of reducing areas that are not covered by bubbles. Furthermore, the position of the center of the stable bubbles is used as the optimal position of cryoprobes in cryosurgery simulation.

TABLE 2. Thermal properties of tissues and blood [21].

Symbol	Parameter	Value	Unit
c_s	specific heat of frozen tumor tissue	1.23	kJ/kg/°C
c_l	specific heat of unfrozen tumor tissue	4.2	kJ/kg/°C
c_b	specific heat of blood	3.64	kJ/kg/°C
k_s	thermal conductivity of frozen tumor tissue	$2.25 \cdot 10^{-3}$	kJ/m/s/°C
k_l	thermal conductivity of unfrozen tumor tissue	$0.55 \cdot 10^{-3}$	kJ/m/s/°C
T_{ml}	liquidus temperature	-1	°C
T_{ms}	solidus temperature	-8	°C
L	latent heat	333	kJ/kg
ρ	density of tumor tissue	1000	kg/m^3
ρ_b	density of blood	1000	kg/m^3
Q_m	metabolic heat generation in tumor	42	kJ/s/m^3
ω_b	blood perfusion in tumor	0.002	ml/s/ml
T_b	temperature of blood	37	°C
T_0	initial temperature	37	°C
T_{probe}	temperature of cryoprobes	-196	°C

TABLE 3. Time needed for -22°C isotherm curve to reach healthy tissues boundary.

Number of cryorobes	t_s (s)	A_{22} (cm^2)	Internal defect (cm^2)	Internal defect (%)
3	126.54	9.918	9.070	47.77
4	99.54	11.423	7.565	39.84
5	98.60	13.323	5.665	29.83
6	57.36	11.340	7.648	40.28
7	53.15	12.233	6.755	35.58
8	55.68	14.377	4.611	24.28
9	60.74	16.162	2.851	15.01
10	37.12	14.339	4.649	24.48

Multiprobe Cryosurgery Simulation

All parameters used in the multiprobe cryosurgery simulation are summarized in Table 2. Domain of the simulation is illustrated in Fig. 1. To obtain accurate results, we consider very small length of subinterval—i.e. $\Delta x = \Delta y = 0.0195313$ cm. Following the stable criterion in (19), we select $\Delta t = 0.00421793$ seconds. At initial, the temperature of both biological tissues and blood is 37 °C. We set up all cryoprobes used in this cryosurgery simulation have the same diameter namely 3 mm. In fact, in real cryosurgery, a cryosurgeon might use combination of several cryoprobes with different diameter. In this simulation, we also assume that there is no change of density during phase transition which results no volume expansion. Cryosurgery process begins when a number of cryoprobes which carry liquid nitrogen with a temperature of -196 °C is inserted into the target region. Then, the temperature surrounding cryoprobes is gradually decreasing until below -22 °C which means that the tumor tissues is damaged. Temperature distribution in biological tissues is calculated by (13) while the -22 °C isotherm curve is computed by plotting the contour of $T(x,y) = -22$ °C.

Suppose t_s is the time required by -22°C isotherm curve to touch the safety boundary of the healthy tissues for the first time. This variable is calculated to determine which cryoprobes layout that give optimal result. The value of t_s for a number of cryoprobes are listed in Table 4. The table shows that if the cryosurgery is terminated before t_s then there will be no healthy tissue damage or in other words if the cryosurgery process is continued exceed t_s then there is a part of healthy tissue damage. Further, we can see that the nine cryoprobes layout have 15.01% of internal defect which is the smallest one than other cryoprobes configuration. Therefore, if a cryosurgeon desires maximum tumor damage without healthy tissues damage then the cryosurgeon should use nine cryoprobes configuration and must terminate the cryosurgery at 60.74 seconds.

As previously discussed that before performing cryosurgery, it is important to consider how many cryoprobes to be used and where the cryoprobes should be inserted into the target region. In addition, the temperature distribution in the

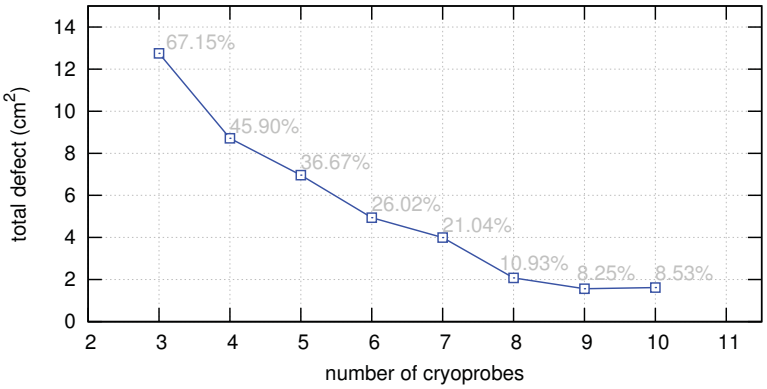

FIGURE 5. Area of total defect with its percentage to target region at $t = 82.67$ seconds.

target region and healthy tissue should be analyzed to determine the deployment of heat in the biological tissues. The temperature distribution and -22°C isotherm curve for multiprobe configurations at $t = 82.67$ seconds are presented in Fig. 6. From that figure, it can be seen that for the three, four, and five cryoprobes configuration, there is no external defect. However, for other cryoprobe configurations, it can be roughly seen that there is increasingly external defect by the decreasing of internal defect. To obtain accurate numerical results, we need to calculate the area of total defect in each cryoprobes configuration.

Area of total defect in the cryosurgery simulation for three to ten cryoprobes configuration is calculated. The simulation for these several configurations are conducted by setting up the same termination time namely 82.67 seconds. Total defect is obtained by previously calculating the area of tissues inside -22°C isotherm curve (denoted by A_{22}). The cryoprobe configuration that has the smallest total defect is an optimal cryosurgery process. Table 4 displays internal, external, and total defect of all cryoprobes configuration at $t = 82.67$ seconds. As can be seen from the table, the internal defect is decreasing with the increment of number of cryoprobes. This is the expected result from our numerical simulation. Moreover, by the increment of number of cryoprobes, the external defect is constantly increasing which is undesired result. But, with complex-shaped geometry of target region is almost impossible to have zero or decreasingly external defect. However, because of decreasingly the internal defect and increasingly the external defect, the total defect could be has minimum with the number of cryprobes is less than ten. Figure 5 reveals the area of total defect with its percentage to a target region for a number of cryoprobes at $t = 82.67$ seconds. As can be seen that the curve in Fig. 5 tends to decrease except at ten cryoprobes. Total defect of ten cryoprobes configuration is 8.53% which is larger than nine cryoprobes configuration (8.25%). Therefore, from this simulation results, it can be said that the optimal lung cancer cryosurgery in this case would be the nine cryoprobes configuration. However, these results depend on the initial bubbles configuration in bubble packing method since with other initial bubbles configurations it might be resulting different results that more optimal.

From the simulation results, we obtain that configuration of nine cryoprobes produces minimum total defect. Figure 7 depicts temperature distribution and evolution of -22°C isotherm curve for nine cryoprobes. As can be seen from the figure, at the time $t = 10.12$ seconds, several ice balls are formed from each probes inserted into the target region. The ice balls have begun to merge to form a single ice region when the diameter of each ice balls reaches approximately 1.26 cm and this occurs at $t = 20.25$ seconds. Moreover, at the time $t = 60.74$ seconds, the -22°C isotherm curve touches the safety boundary of healthy tissue with internal defect of 15.01%. If it is desired the healthy tissues have 0% damage then the cryosurgery process can be stopped at this time but there is still risk about 15.01% of tumor tissues which has not been destroyed. At $t = 82.67$ seconds, the nine cryoprobes configuration has internal defect of 5.95% and external defects of 2.30%. To prevent excessive damage to healthy tissue, a cryosurgeon could decide that cryosurgery should be discontinued at $t = 82.67$ seconds with 5.95% of tumor tissues has not died. It may be decided by cryosurgeon that the rest 5.95% of tumor tissues can be destroyed in the next other cryosurgery planning.

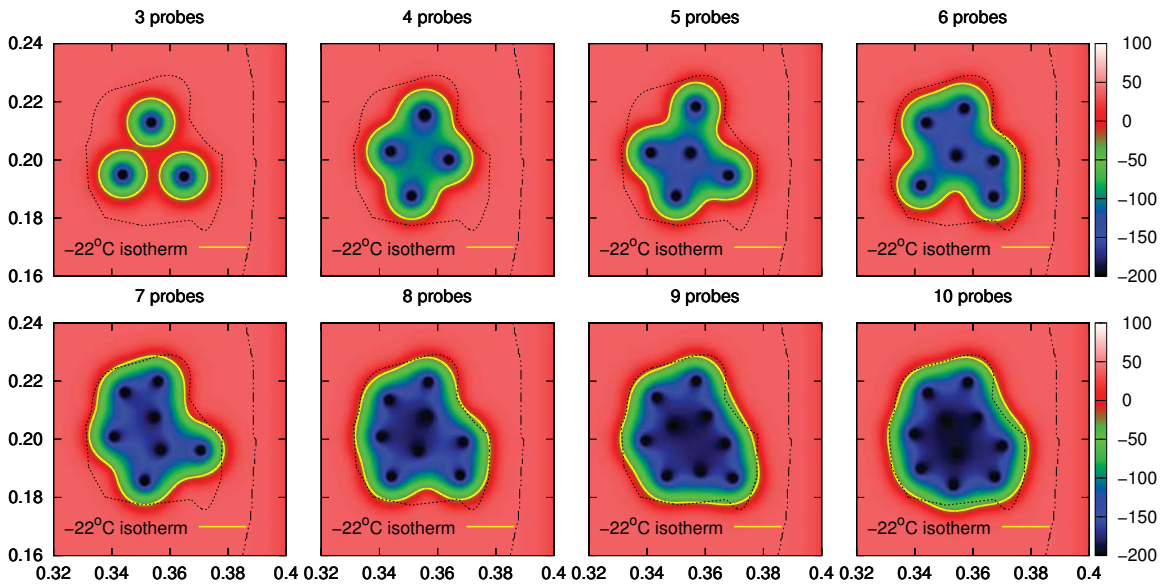

FIGURE 6. Temperature distribution and $-22°C$ isotherm curve of multiprobe cryosurgery at $t = 82.67$ seconds. Image order from top left to bottom right: multiprobe cryosurgery using 3, 4, ... , and 10 cryoprobes.

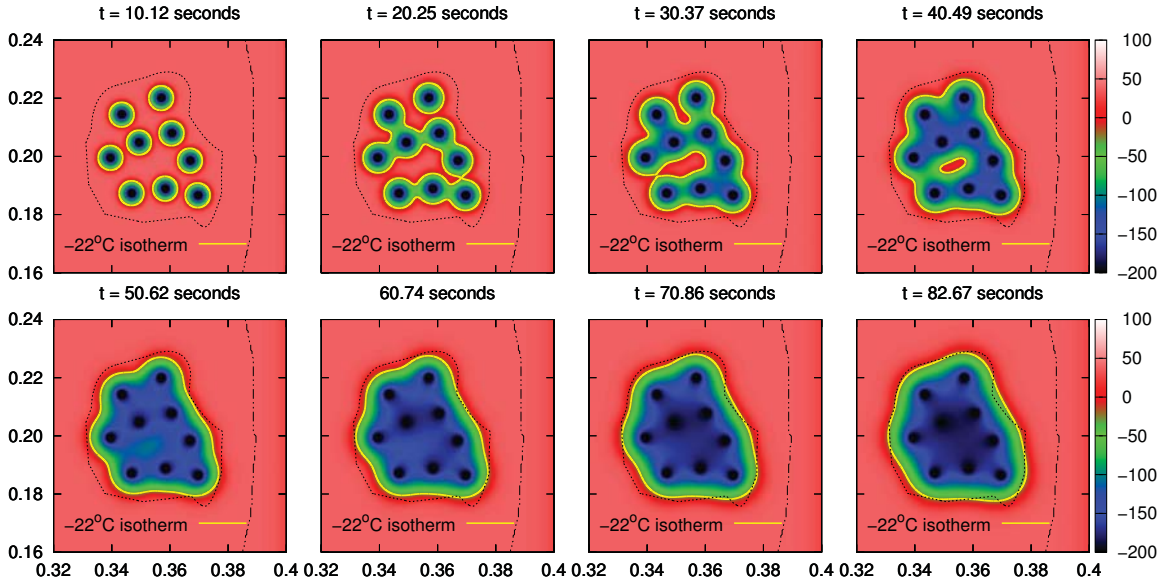

FIGURE 7. Temperature distribution and $-22°C$ isotherm of multiprobe cryosurgery using 9 cryoprobes. Image order from top left to bottom right: $t = 10.12$, $t = 20.25$, $t = 30.37$, $t = 40.49$, $t = 50.62$, $t = 60.74$, $t = 70.86$, $t = 82.67$ seconds.

CONCLUSION

Multiprobe cryosurgery with complex-shaped tumors has been successfully simulated using Godunov method where the optimal cryoprobes configuration obtained from stable bubbles position of bubble packing method. Total defect of target region for three to ten optimal cryoprobes layout has been analyzed to find maximum cryoinjury of tumor tissue

TABLE 4. Numerical results of 2D cryosurgery simulation at $t = 82.67$ seconds where A_{22} is area of tissues that have temperature below -22°C.

Number of cryorobes	A_{22} (cm^2)	Internal defect (cm^2)	External defect (cm^2)	Total defect (cm^2)
3	6.238	12.750	0.000	12.750
4	10.273	8.715	0.000	8.715
5	12.025	6.963	0.000	6.963
6	14.086	4.921	0.019	4.940
7	15.283	3.850	0.145	3.995
8	17.204	1.930	0.146	2.076
9	18.295	1.130	0.436	1.566
10	19.364	0.622	0.998	1.620

and minimum healthy tissue damage. It has be shown that the nine cryoprobes configuration has the smallest total defect about 8.25% for cryosurgery duration 82.67 seconds. Further, time needed for -22°C isotherm to reach safety boundary of healthy tissues depends on cryoprobes position and degree of complex geometry of target region. For the nine cryoprobes, time required for a surgeon to conduct cryosurgery with maximum tumor damage (approximately 84.95%) but without healthy tissues damage is 60.74 seconds. However, if the cryosurgeon desires to take risk, the cryosurgery may be continued until 82.67 seconds with cryoinjury of tumor tissues about 94.05% and healthy tissues damage approximately 2.30%. These numerical results are highly suggested to be considered in multiprobe cryosurgery planning so that the objective of cryosurgery can be achieved. Suggestion to future research is to develop multiprobe cryosurgery simulation using real cancer geometry and combination of different cryoprobes diameter. To obtain more real results, it may develop to three-dimensional simulations and validate the results with experimental data.

REFERENCES

1. K. J. Chua, *Computers in Biology and Medicine* **41**, 493–505 (2011).
2. M. R. Rossi, D. Tanaka, K. Shimada, and Y. Rabin, *International Journal of Heat and Mass Transfer* **51**, 5671–5678 (2008).
3. M. R. Rossi, D. Tanaka, K. Shimada, and Y. Rabin, *Computer Methods and Programs in Biomedicine* **85**, 41–50 (2007).
4. D. C. Lung, T. F. Stahovich, and R. Rabin, *Computer Methods in Biomechanic and Biomedical Engineering* **7**, 101–110 (2004).
5. R. G. Keanini and B. Rubinsky, *Journal of Heat Transfer* **114**, 796–801 (1992).
6. D. Tanaka, K. Shimada, and Y. Rabin, *Journal of Biomechanical Engineering* **128**, 49–58 (2006).
7. G. Giorgi, L. Avalle, M. Brignone, M. Piana, and G. Caviglia, *Computer Methods in Biomechanics and Biomedical Engineering* **16**, 885–895 (2013).
8. A. Kumar, *Heat Mass Transfer* **50**, 1751–1764 (2014).
9. R. Wan, Z. Liu, K. Muldrew, and J. Rewcastle, *Computer Methods in Biomechanics and Biomedical Engineering* **6**, 197–208 (2003).
10. H. H. Pennes, *Journal of Applied Physics* **1**, 93–122 (1948).
11. V. Alexiades and A. D. Solomon, *Mathematical Modeling of Melting and Freezing Processes*, Hemisphere Publishing Corporation, Washington DC, 1981.
12. J. Caldwell and Y.Y. Kwan, *Communications in Numerical Methods in Engineering* **20**, 535–545 (2004).
13. V. Voller and M. Cross, *International Journal of Heat and Mass Transfer* **24**, 545–556 (1981).
14. V.R. Voller and L. Shadabi, *International Communications in Heat and Mass Transfer* **11**, 239–249 (1984).
15. A. Esen and S. Kutluay, *Applied Mathematics and Computation* **148**, 321–329 (2004).
16. D. Tarwidi, and S. R. Pudjaprasetya, *East Asian Journal of Applied Mathematics* **3**, 107–119 (2013).
17. R.J. Leveque, *Finite-Volume Methods for Hyperbolic Problems*, Cambridge University Press, Cambridge, 2002.
18. K. J. Chua, S. K. Chou, and J. C. Ho, *Journal of Biomechanics* **40**, 100–116 (2007).
19. T. Shih, P. Yuan, W. Lin, and H. Kou, *Medical Engineering & Physics* **29**, 946–953 (2007).
20. Z. Deng and J. Liu, *Journal of Biomedical Engineering* **124**, 638–649 (2002).
21. S. Kumar and V. K. Katiyar, *International Journal of Applied Mathematics and Mechanics* **3**, 1–17 (2007).
22. R.I. Andrushkiw, *Mathl. Comput. Modelling* **13**, 1–9 (1990).
23. K. Shimada,*Physically-Based Mesh Generation: Automated Triangulation of Surfaces and Volumes via Bubble Packing*, PhD Thesis, Massachusetts Institute of Technology, Cambridge, MA, 1993.
24. N. Qi, Y. Nie, and W. Zhang, *Commun. Comput. Phys* **16**, 115–135 (2014).